Valence bond solid state induced by impurity frustration in Cr_8Ni

J. Almeida, M. A. Martin-Delgado, and G. Sierra
Departamento de Física Teórica I, Universidad Complutense, 28040 Madrid, Spain and Instituto de Física Teórica, C.S.I.C.-U.A.M., Madrid, Spain 28049

(Received 20 October 2008; revised manuscript received 13 January 2009; published 31 March 2009)

We provide a physically meaningful picture of the nature of the ground state of the Cr_8Ni compound in the regime where it is a spin singlet. According to this picture, the anisotropy of the Ni atom in the Cr ring induces a dimerization in the molecule that makes the ground state to stabilize in a valence bond solid phase of virtual spins. We characterize rigorously this phase by means of a particular nonlocal order parameter that denoted the generalized string order parameter. In the completely antiferromagnetic regime, the system becomes frustrated. We have performed a numerical real-time evolution study of the correlations between the spin of the Ni impurity and the rest of the spins in order to show the reaction of the system under this frustration.

DOI: 10.1103/PhysRevB.79.115141 PACS number(s): 75.10.Jm, 75.50.−y, 74.20.Mn

I. INTRODUCTION

Recently, the physics of ring-shaped molecular magnets, with antiferromagnetic interactions and an odd number of interacting spin centers (e.g., paramagnetic ions), has attracted a great deal of interest since they provide emblematic examples of systems where spin frustration effects due to quantum magnetism play a major role. Moreover, they have been synthesized and studied experimentally.[1–5] Specifically, we shall concentrate on the anomalous magnetic properties in some heterometallic odd spin rings,[6–9] namely, chromium rings. The system comprises eight chromium(III) ions with spin $S=\frac{3}{2}$ each and one nickel(II) ion with spin $S=1$. The magnetic properties of this first odd-member antiferromagnetic ring have been investigated with electron paramagnetic resonance (EPR), and its spin frustrated properties have been visualized by means of a Möbius strip. In this paper we propose an alternative and complementary picture of the ground state of this Cr_8Ni ring molecule using valence bond states (VBS) (Refs. 10–18) of virtual spins which are used to represent the spins $S=\frac{3}{2},1$ of the real constituent ions. We will show that the particular bond pattern acquired by these VBS states is a consequence and manifestation of the spin frustration in the odd Cr_8Ni ring molecule.

Molecular nanomagnets are fascinating new magnetic materials.[19–21] They appear in a large variety of compounds with many different properties. We shall focus on antiferromagnetic compounds of bimetallic rings. These molecules are ideal candidates to study the physics of simple but nontrivial spin models such as the AF Heisenberg interaction. The key point here is that these molecules show very interesting finite-size quantum many-body effects which are typically overlooked in other studies of the Heisenberg model where the main focus is to achieve the thermodynamic limit (number of spins going to infinity). In those studies, the small finite-size effects are considered spurious effects that vanish for larger and larger systems, which eventually may show some sort of universality, if that is the case. Quite on the contrary, the nice thing about these small molecules is that we can vary their size and coupling constant strengths such that the finite-size effects become some real property that can be addressed experimentally, theoretically, and numerically. Some interesting examples of these small quantum effects that we study in this paper are level crossing, change in the nature of their the ground state (e.g., from spin singlet to spin triplet or higher), existence of excited states very close to the ground state, etc.

In Sec. II we introduce a Heisenberg Hamiltonian to describe the interactions between the two types of ions in the bimetallic compound Cr_8Ni, where the Ni ion plays the role of an impurity within an homogeneous chain of Cr ions with the shape of a ring molecule. In Fig. 1 we present the energy spectrum of this Hamiltonian obtained numerically with an appropriate Lanczos technique. In Sec. III, we first provide the VBS picture for the Cr_8Ni ring molecule based on a strong coupling limit in the Ni impurity coupling. This is the origin of the spin frustration in the system. In order to support this VBS picture, we provide numerical results for a generalized string order parameter (SOP) that is able to detect the type of virtual bond structure. In Sec. IV we study

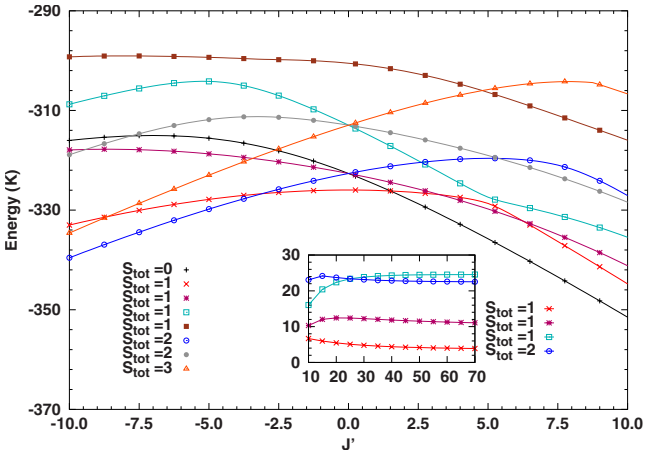

FIG. 1. (Color online) Energy spectrum of some of the lowest lying states in each sector with well-defined total spin. In the coupling region shown, the spectrum is highly dependent on the values of J and J'. In particular, in the antiferromagnetic region $J'>0$ K the ground state is a triplet for $J'<1.5$ K and a singlet elsewhere. Inset: energy gap as a function of J' from the singlet ground state to the first excited states. The legend shows the total spin of each of these excited states.

the frustration effects in this ring molecule by means of a numerical study of time-evolved correlation functions of spin-spin operators for different ions in the nanomolecule. Sec. V is devoted to conclusions.

II. HAMILTONIAN DESCRIPTION OF THE Cr_8Ni MOLECULE RING

Magnetic molecules are emblematic instances of an ensemble of noninteracting quantum systems embedded in a condensed matter environment. The synthesis of molecular magnets has undergone rapid progress in recent years. Each of those quantum systems are identical molecular units that can contain as few as two and up to several dozens of paramagnetic ions (spins). In our case, they correspond to Cr_8Ni ring molecules. This molecule is one of the many relevant molecules containing transition-metal ions whose spins are so strongly exchange coupled that when the temperature is low enough, their behavior is like single-domain particles with a certain total spin.[19–21]

Macroscopically, these materials appear as crystals or powders. Nonetheless, their intermolecular magnetic interactions are utterly negligible when compared to their intramolecular interactions. Thus, measurements of their magnetic properties reflect mainly ensemble properties of single molecules. There are two major advantages in the research on these molecule aggregates. First, the outstanding degree of accuracy by which their magnetic dynamics can usually be modeled; second, the opportunity to chemically engineer molecules possessing desired physical properties.[19–21] In our case, the interest relies on the study of the Heisenberg model in situations that are usually discarded when studying that model in infinite one-, two-, and three-dimensional systems. Our studies will reinforce the idea that such spin arrays yield physics caused by the finite size of the system.

The Cr_8Ni compound belongs to a wider family of molecular rings. In molecules with a small number of ions, there exist big differences in their physics depending on each particular compound. A first major difference is related to the number of its ions: odd or even. In this regard, the implications are mainly twofold: first, having a difference of one ion in the same family of molecules can cause the molecule to have a neat magnetic moment or not, therefore changing its magnetic properties drastically. Second, and interestingly enough, a molecular ring with completely antiferromagnetic interactions between nearest-neighbor ions can be a candidate to present quantum spin frustration properties if the number of atoms is odd, while this effect will not generally be present for even member rings in a given family compound.

As it happens, in the majority of these molecules the localized single-particle magnetic moments of the ions couple antiferromagnetically. Then, their spectrum is described rather well by the Heisenberg model with very few parameters because of the high symmetry of the molecular configurations. These coupling parameters correspond to isotropic nearest-neighbor interaction sometimes augmented by anisotropy terms.

The Cr_8Ni compound is one of the first antiferromagnetic odd-member rings which has been artificially synthesized. The results of its magnetic properties are interpreted within the framework of a spin Hamiltonian approach, and they nicely fit the pattern of the energy levels obtained by inelastic neutron spectroscopy. There exist also reports on its magnetic and spin frustration effects.[7] In view of these properties, it has been proposed[1] that the behavior of this molecule can be properly explained with a nearest-neighbor Heisenberg model where only two different microscopic couplings play a role: one is the coupling that parametrizes the strength of the interaction existing between the Ni and the neighbor pair of Cr. The other one is the coupling that takes into account the interaction between the Cr-Cr pairs, which can be considered the same for each pair. The easy-axis anisotropy term is reported to be very weak now as to play any role. Therefore, the Hamiltonian that we shall study has the following form:

$$H = J\sum_{i=1}^{7} \mathbf{S}_{\mathrm{Cr}}(i)\cdot\mathbf{S}_{\mathrm{Cr}}(i+1) + J'[\mathbf{S}_{\mathrm{Ni}}\cdot\mathbf{S}_{\mathrm{Cr}}(1) + \mathbf{S}_{\mathrm{Ni}}\cdot\mathbf{S}_{\mathrm{Cr}}(8)], \tag{1}$$

where, for convenience, the Cr atoms have been numbered from 1 to 8, these latter being the two neighbors of the Ni atom. Notice that since the spin of the Ni is equal to $\mathbf{S}_{\mathrm{Ni}}=1$ and the spin of the Cr atoms is $\mathbf{S}_{\mathrm{Cr}}=3/2$, the total spin of the molecule must be integer.

In Fig. 1 we have plotted some lowest lying energy levels of this Hamiltonian. In Sec. IV we shall explain how these numerical results have been obtained with a multitarget Lanczos method. It can be observed that in some regime of the coupling constants J' and J, the energy levels are highly braided and, as a consequence, the ground state has different value of the total spin depending on the exact value of these couplings. However, as can be seen from the inset of this figure, for large values of J' the ground state is always a spin singlet with a triplet state very close in energy above it. In this work, we will restrict our study to the antiferromagnetic $(J'>0)$ region and in particular to the region where the ground state is a singlet. From Fig. 1 we see that this area corresponds to $J'>1.5$ K, while the region $0<J'<1.5$ K is characterized by a ground state with total spin equal to one (for convenience the computations in Fig. 1 have been done with a fixed value of $J=16$ K).

The interest in the domain where the ground state is a singlet comes not only from the fact that it spans the most extension in the antiferromagnetic area but also because the physics of the real Cr_8Ni seems to be in agreement with a regime close to $J=16$ K and $J'=70$ K, with a nonmagnetic ground state. Therefore, the interest of our study relies on the fact that it can provide insights into the physics of a not so well-known state of matter but with a well-defined connection with experiments in real compounds.

III. IMPURITY INDUCED VBS PICTURE

A valence bond solid is a particular quantum many-body state that can be understood as follows: given a system of *real* particles with total spin S, we can split each one of them into $2S$ *virtual* particles of spin $S=1/2$. In order to recover

the original spins, we enforce these virtual particles to couple (i.e., symmetrize) among themselves in order to give the original spin S particles. To create now a wave function with total spin equal to zero, we make singlets (i.e., antisymmetrize) out of every pair of virtual particles.

We will denote each of these singlet pairs between virtual particles as a bond. There are a lot of different possible ways to fix the bonds between all the virtual particles and, in general, the total wave function may have contributions from all these configurations. There exist however some physical situations in which only some particular bond configurations, out of the whole possible set, take part in the wave function: some systems have a major contribution coming only from one particular bond arrangement. These systems are commonly dubbed as bond crystals. It may also happen that there exist not one but some few bonds configurations whose weights are dominant in the total wave function. In this case the system is called a resonating valence bond solid (RVBS). There exists yet another kind of more disordered states, denoted (m,n)-VBS, which we shall see that describe properly the ground state of the Cr_8Ni in the singlet region. A general (m,n)-VBS state is built by forming bonds only between virtual spins belonging to neighbor real particles, with the numbers m,n satisfying $m+n=2S$ and S being the spin of the real particle.

These states are usually translationally invariant [with the (m,n)-VBS notation this means that $m=n$] in those systems where the Hamiltonian possesses this symmetry. There also exist dimerized (m,n)-VBS states that have been shown to appear in systems where the full translational symmetry of the Hamiltonian has been partially broken such that still exists an enlarged unit cell. Typically, this effect can be obtained by introducing an external dimerization coupling constant in the Hamiltonian that still preserves some periodicity.

Our main result in this section is that there is another mechanism to provide such dimerized (m,n)-VBS states in the Cr_8Ni ring molecule and whose success precisely resides in the existence of an impurity within an homogeneous system. To understand this mechanism in the particular case of the Cr_8Ni, we resort to the strong coupling limit where the antiferromagnetic interaction between the Ni and its neighbors is much larger that the interaction among Cr pairs. As shown in Fig. 2, the two virtual spins comprising the Ni will be likely to form bonds with the virtual particles in the neighbor chromiums to satisfy their antiferromagnetic constraints. The rest of the virtual spins left will then tend to form similar bonds with their neighbor partners, giving as a result a dimerized non translationally invariant VBS. We would like to stress the fact that the validity of this picture is rooted in the existence of the Ni impurity. In fact, the physics of a homogeneous system of Cr atoms is closer to a gapless critical phase rather than to such a gapped state.

General (m,n)-VBS states belong to a class of spin liquids which are known to possess an special hidden order that can be identified by a particular nonlocal order parameter called the SOP.[22–27] This order parameter has proven itself extremely successful in the task of characterizing diverse kinds of such states, both in the pure one dimensional cases and also in less trivial systems such as ladders.[25,27] We shall see that this parameter also allows us to characterize the

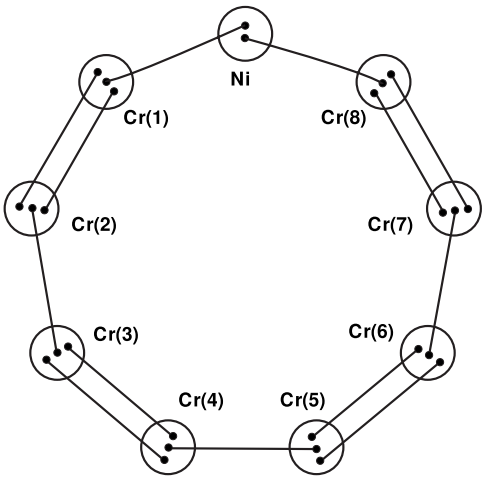

FIG. 2. Valence bond solid picture of the Cr_8Ni ring molecule. The bonds established between the two virtual spins in the Ni and the two virtual spins in the neighbor Cr atoms force a dimerized pattern in the rest of the chain. This VBS configuration becomes the dominant one in the strongly coupled impurity limit $J' \gg J$.

Cr_8Ni ground state. The definition of the generalized string order parameter is as follows:[24]

$$O_{\mathrm{str}}(\theta) = \lim_{|j-i|\to\infty} \left\langle S_i^z \exp\left(i\theta \sum_{k=i}^{j-1} S_k^z \right) S_j^z \right\rangle, \qquad (2)$$

where both $i=2k\pm 1$ and $j=2k'\pm 1$. That is, i and j are both either odd or even. With this definition the dependence on θ of the string order parameter acting upon an ideal infinite sized (m,n)-VBS can be exactly computed[24] using the standard Schwinger bosons representation. We hereby summarize some general properties of this parameter. The first two ones are formal and contain practical information; the last ones are those which actually equip the SOP with the powerful capability to determine and characterize valence bond solids:

(i) the SOP is symmetric with respect $\theta=\pi$.

(ii) In states with time-reversal symmetry, that is, invariant under the operation $S_i^z \to -S_i^z$, the SOP is a real number.

(iii) Given a generic (m,n)-VBS state, the number of zeros of this operator in the interval $\theta \in [0,2\pi)$ coincides with the number m.

(iv) Two measures of the SOP beginning in adjacent sites will differ in the order of the numbers m and n. That is, if one measure gives a (m,n)-VBS state, the other will be a (n,m)-VBS.

In Fig. 3 we have plotted the form of the SOP in an ideal infinite (1,2)-VBS and a (2,1)-VBS. Notice that all the properties above hold true and that the shape itself of the SOP is unique and characteristic of each valence bond solid. In particular these two cases will be useful later for comparison with the SOP computed in the finite molecule.

In the rest of the section we will check the valence bond solid nature of the Cr_8Ni molecule. However, there is a subtle point that must be addressed before moving on to this task: the θ dependence of the SOP as well as the related properties written above can be only rigorously derived in

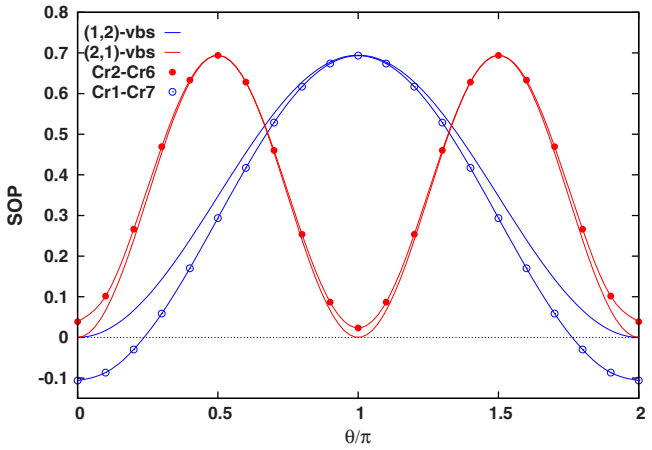

FIG. 3. (Color online) The curves with no symbols represent the string order parameter for an ideal (1,2)-VBS and (2,1)-VBS with infinite size. The curves with symbols represent the string order parameter $O_{\mathrm{str}}(\theta,i,j)$ computed in the VBS of Eq. (3) for two different configurations: i and j corresponding to the sites of the Cr_1 and Cr_7 (solid circles) and to the sites of the Cr_2 and Cr_6 (empty circles).

ideal VBSs with infinite sizes. It must be checked that the behavior of this operator in the VBS represented in Fig. 2 preserves the expected properties. To face this task we will use the standard Schwinger bosons representation, which is particularly well suited to compute matrix elements of spin operators in valence bond solids. In this representation the (un-normalized) wave function of the VBS corresponding to Fig. 2 can be written as

$$|\mathrm{vbs}\rangle = (a_0^\dagger b_1^\dagger - b_0^\dagger a_1^\dagger)(a_1^\dagger b_2^\dagger - b_1^\dagger a_2^\dagger)^2(a_2^\dagger b_3^\dagger - b_2^\dagger a_3^\dagger)(a_3^\dagger b_4^\dagger - b_3^\dagger a_4^\dagger)^2(a_4^\dagger b_5^\dagger - b_4^\dagger a_5^\dagger)(a_5^\dagger b_6^\dagger - b_5^\dagger a_6^\dagger)^2(a_6^\dagger b_7^\dagger - b_6^\dagger a_7^\dagger)(a_7^\dagger b_8^\dagger - b_7^\dagger a_8^\dagger)^2(a_8^\dagger b_0^\dagger - b_8^\dagger a_0^\dagger)|0\rangle, \quad (3)$$

with the notation that the subindex zero refers to the Ni atom and the rest stands for each of the Cr ones. It can be observed that all the terms of this wave function belong to a restricted subspace of the total Fock space where the Bose occupation numbers $n_i^a + n_i^b$ are twice the value of the total spin S_i. This fact ensures that the wave function is an eigenstate of each local spin operator $\mathbf{S}_i$; that is, the symmetrization of virtual particles is implicit in this representation. On the other hand, the terms within parentheses create a rotationally invariant bond between adjacent particles. Since the number of particles involved in this state is small, the limit $|j-i| \to \infty$ in definition (2) is meaningless, and we will treat the numbers i and j as free parameters. This freedom will allow us to compute the SOP using different blocks of particles (see Fig. 4) to check property (iv). With these considerations in mind the expression to compute the string order parameter in the ideal VBS of Eq. (3) is

$$O_{\mathrm{str}}(\theta,i,j) = \frac{\langle \mathrm{vbs}|S_i^z \exp\left(i\theta \sum_{k=i}^{j-1} S_k^z\right) S_j^z|\mathrm{vbs}\rangle}{\langle \mathrm{vbs}|\mathrm{vbs}\rangle} \quad (4)$$

Notice that both the numerator and denominator of this expression give raise to a number of sums that is exponential

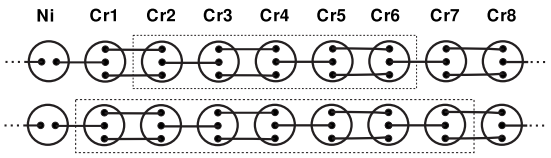

FIG. 4. Representation of two ways to measure the SOP in the Cr_8Ni ring choosing adjacent starting sites. In the diagram at the top we break two bonds at the left end and one at the right. This corresponds to a (2,1)-VBS. In the diagram at the bottom we have the same physical configuration but now we are breaking one bond at the left and two at the right end, which characterizes a (1,2)-VBS.

with the number of bonds of the wave function. With the use of a computer and careful implementation, each mean value can be obtained from the contribution of two[26] terms (the product of 10^{13} from the wave-function definition and 10^{13} from its Hermitian conjugate). (The action of the operators of the string order parameter can be absorbed in these terms.) Moreover, we have checked with our program that in general less than 1% of the total number of terms contributes a value different from zero, which simplifies significantly the calculation. In Fig. 3 we have plotted the string order parameter computed in the ideal state of Eq. (3). It can be seen in this figure that the properties of the SOP described above clearly hold in this small system and, most important, that the characteristic shape of this parameter is almost identically preserved. One important difference can be observed however and it is precisely at the points $\theta=0,2\pi$ (at these points the SOP is a usual spin-spin correlator) that the SOP in the finite case does not vanish but shows a certain correlation, while in larger systems this value decays to zero.

Now that we are familiar with the SOP in ideal valence bond solids we will perform an analogous study with the more realistic Cr_8Ni molecule described by Hamiltonian (1). In Fig. 5 we have plotted the SOP computed in the ground state of this Hamiltonian with the different configurations shown in Fig. 4. Since the ground state is a singlet and due to property (ii) the imaginary parts vanish in all our computations.

In Fig. 5(a) the curves with high values of J' have two local minima in the interval $\theta \in [0,2\pi)$ whose value is compatible with zero considering that the system is finite. This result is consistent with a (2,1)-VBS. The shape of the SOP is also typical of these states, with two noticeable maxima placed approximately at $\theta=\pi/2$ and $\theta=3\pi/2$. Accordingly, the computations shown in Fig. 5(b) shall be consistent with a (1,2)-VBS as explained above. We see that the shape of the SOP for the strong coupling curves shares again the main features of these states, that is, one substantial maximum placed precisely at $\theta=\pi$. In this case however magnified spin-spin correlations appear at $\theta=0,2\pi$ if we compare them with the same computation on the ideal state (Fig. 3). This increase results naturally, taking into account that the valence bond solid state in the real molecule appears as a consequence of the antiferromagnetic interaction of the impurity. The high correlation between spins close to the impurity is then a necessary payoff to stabilize the ground state in a global valence bond solid.

In summary, the string order parameter reveals that the ground state of the Cr_8Ni in the strong impurity coupling

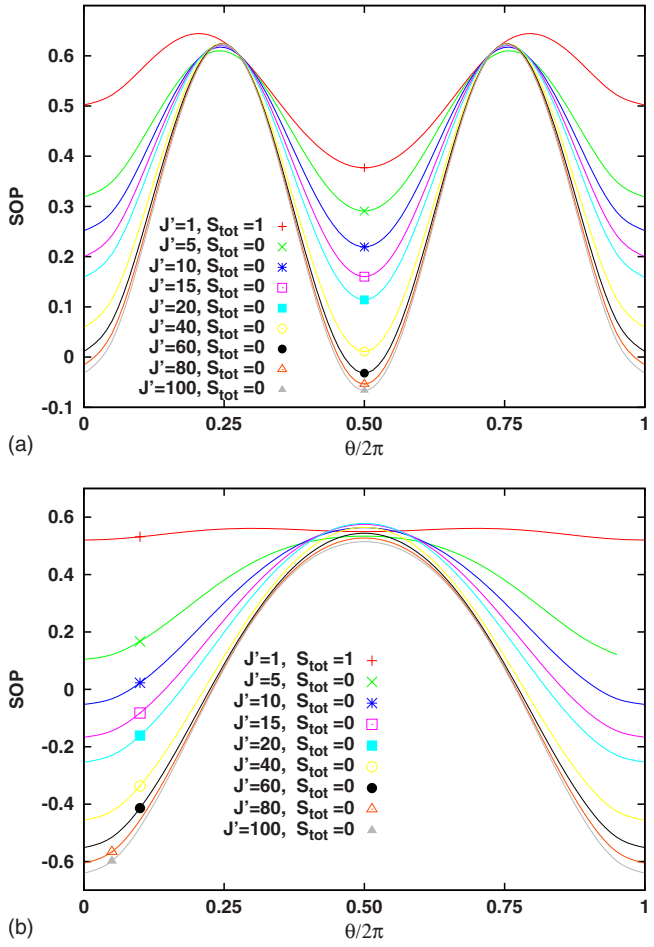

FIG. 5. (Color online) (a) SOP computed between the Cr_2 and the Cr_6 atoms. (b) SOP computed between the Cr_1 and the Cr_7 atoms. We have fixed $J=16$. Considering the interval $\theta \in [0, 2\pi)$ and looking at the curves with high values of J' we see that the number of zeros in (a) is two, corresponding to a (2,1)-VBS. In (b) the situation is more confusing due to stronger finite-size effects that shift the curves toward negative values at $\theta=0$ and $\theta=\pi$. With this correction in mind the graph strongly suggests the existence of a (1,2)-VBS.

limit is consistent with an impurity-mediated mechanism of spin frustration, the result of which is the dominant and global VBS pattern shown in Fig. 2 affected by some local correlations that appear as a consequence of the finite size of the system. In finite systems the possibilities to drastically change the nature of the ground state are limited; that is, the possibility of a quantum phase transition is excluded and only a crossing with another energy level can produce this effect. Therefore, the intermediate J'/J regime can be considered as some deformation of the strong coupling limit. As we decrease J' and the $S_{\text{tot}}=1$ state crosses the $S_{\text{tot}}=0$, the VBS picture breaks down and the measures of the SOP are not meaningful in the sense that the properties of this operator in such a state are not well defined.

To conclude this section it is worth mentioning the fact that the quantum configuration of the Cr_8Ni is a valence bond solid includes this molecule in a wider family of compounds with many representatives in the form of one-dimensional spin chains and spin ladders. Restricting ourselves to the former group there exist many candidates as valence bond solids within the NENP, NTENP, and NDMAP compound families. In particular for some of these materials there exist experimental studies (Ref. 28 and references therein) that make use of magnetization, electron-spin resonance, and inelastic neutron-scattering techniques to study the properties of the underlying valence bond solid structures. To the best of our knowledge the Cr_8Ni is among the first ring-shaped valence bond solids that can actually be synthesized. We expect however that some of the experimental facts and techniques employed for other VBS compounds can be also adopted for this material.

IV. FRUSTRATION AND DYNAMICS IN Cr_8Ni

As we have already mentioned, the Cr_8Ni ring molecule is frustrated in the sense that the minimum energy of the system cannot be obtained minimizing separately each of the two body terms of Hamiltonian (1). Another way to see it is by resorting to the classical limit where each spin is pictured as a classical vector. Once we set the value of one of those classical spins, then we can fix one by one the rest of the spins in order to minimize the local interactions. But in the end there will be one spin for which the local interaction with both of its neighbors cannot be minimized at the same time.

Typically, systems where frustration exists come along with a rich and very often not so well-known physics. Roughly speaking, we can say that frustration in general increases the complexity of those systems, both in the physics they exhibit as well as in the way to approach them. In particular, there is not a well-defined way to measure the amount and localization of frustration. An attempt to quantify these effects in Cr_8Ni can be done attending to the structural changes in the ground state as we vary the couplings, that is, by inspection of the way in which spins in the ring couple to form the final state. This procedure has a connection with experimental techniques where the Lande factors of the ring can be measured. However this procedure is not suitable to study a rotationally invariant singlet ground state where the spin is zero. In this section we will study the behavior of the Cr_8Ni molecule by means of computing the time evolution of some important spin correlators: the spin autocorrelation of the impurity Ni atom with itself and the spin correlation between the Ni atoms and each Cr along the ring. These correlators correspond to the vacuum expectation value of the time-evolved spin operators $\mathbf{S}_{\text{Ni}}(t)$ and $\mathbf{S}_{\text{Cr}_i}(t)$ projected onto the spin operator of the Ni impurity at $t=0$, $\mathbf{S}_{\text{Ni}}(0)$. This is a way to dynamically probe[29–33] the spin structure in the ground state $|\psi_0\rangle$ of the ring molecule. In fact, we shall consider the square modulus of those correlators and interpret them as time-evolution probabilities. That is, we shall consider the following correlators in order to construct a figure of merit:

$$C_{\text{Ni}}(t) := \langle \psi_0 | \mathbf{S}_{\text{Ni}}(t) \cdot \mathbf{S}_{\text{Ni}}(0) | \psi_0 \rangle, \tag{5}$$

and

$$C_{\mathrm{Cr}_i}(t) := \langle\psi_0|\mathbf{S}_{\mathrm{Cr}_i}(t)\cdot\mathbf{S}_{\mathrm{Ni}}(0)|\psi_0\rangle. \quad (6)$$

Notice that in a rotationally invariant singlet ground state $|\psi_0\rangle$ the correlations in the x,y and z axes have the same value, and thus, the expressions above can be written as

$$C_{\mathrm{Ni}}(t) = 3\langle\psi_0|S^z_{\mathrm{Ni}}(t)S^z_{\mathrm{Ni}}(0)|\psi_0\rangle, \quad (7)$$

$$C_{\mathrm{Cr}_i}(t) = 3\langle\psi_0|S^z_{\mathrm{Cr}_i}(t)S^z_{\mathrm{Ni}}(0)|\psi_0\rangle. \quad (8)$$

Since the proportionality factor does not provide any additional information we will discard it from now on and will consider the bare z-axis projection correlators. The time dependency of the operators is given by the usual Heisenberg picture,

$$O(t) = e^{iHt}O(0)e^{-iHt}. \quad (9)$$

The idea behind this figure of merit to measure the dynamical correlations between spins is similar to the static correlator used to measure spin correlations in space separated sites i and j of the ring $\langle\psi_0|\mathbf{S}_{\mathrm{Cr}_i}(i)\cdot\mathbf{S}_{\mathrm{Ni}}(j)|\psi_0\rangle$. This static correlator measures spatial correlations, while our purpose is to measure time-evolved correlations which will probe not only the ground state physics but also the excited states physics.

We next explain briefly the numerical method used to evaluate these correlators. After that we shall show and discuss the results.

A. Numerical method

Hamiltonian (1) is $SU(2)$ rotational invariant. That is, it commutes both with the total spin and the z-axis projection of the total spin. In Table I we show the dimensions of the subspaces corresponding to the conserved quantum numbers of these operators. These sizes are in the limit to perform exact diagonalization but lie however within the domain reachable for a Lanczos method.

To do our computations we will make use of an adapted version of the Lanczos algorithm specific to compute real-time dynamics.[34–36] In this framework it can be shown that the correlators written above can be expressed as

$$C_i(t) = \sum_{j=0}^{M}\langle\psi_0|S^z_{\mathrm{Cr}(i)}(t)S^z_{\mathrm{Ni}}(0)|\tilde{\psi}_j\rangle\langle\tilde{\psi}_j|S^z_{\mathrm{Ni}}(0)|\psi_0\rangle e^{-i(\tilde{\epsilon}_j-E_0)t}, \quad (10)$$

where M stands for the dimension of the Krylov space $\mathcal{K}(H,q_0,M)$ such that $\mathcal{K}(H,q_0,M)=\mathcal{K}(H,q_0,M+1)$, with $q_0 := S^z_{\mathrm{Ni}}|\psi_0\rangle$. That is, M is the dimension of the largest invariant subspace generated by successive applications of the Hamiltonian H upon the seed vector $q_0=S^z_{\mathrm{Ni}}|\psi_0\rangle$. The vectors $|\tilde{\psi}_j\rangle$ are the approximated eigenvectors computed in this Krylov subspace, $\tilde{\epsilon}_j$ are the energies of these eigenvectors, and E_0 stands for the energy of the ground state.

The number M is typically much lower than the total dimension of the Hilbert space but still high to numerically compute a complete basis of the Krylov subspace. Therefore, the approximation in this method resides in the fact that we will substitute the dimension M with a lower number of vectors that still serve as a complete basis for these correlators.

TABLE I. Dimension of each subspace with well-defined quantum numbers out of the total Hilbert space of a Cr_8Ni ring. The second column corresponds to the subspaces with well-defined total spin. The third one are the sectors with well-defined value of the z-axis projection of the total spin. In this last case for each value in the first column we must consider the positive and negative cases.

$\mathbf{S}_{\mathrm{tot}}, \pm S^z_{\mathrm{tot}}$	Dimension	Dimension
0	1000	23548
1	2764	22548
2	3905	19784
3	4256	15879
4	3900	11623
5	3095	7723
6	2150	4628
7	1308	2478
8	692	1170
9	314	478
10	119	164
11	36	45
12	8	9
13	1	1
Total:	196608	196608

In order to obtain the most accurate results and representations of the eigenvectors of the Hamiltonian $|\tilde{\psi}_j\rangle$, we have not used the same Krylov space to compute them all. Instead we have performed a Lanczos iteration to find the ground state. After that, the Lanczos iteration is restarted with the previously found eigenvectors projected out of the subspace to find the next excited state, and so on and so forth until we have computed the desired number of eigenvectors. In particular, to compute the correlators described before we have used 400 eigenvectors of the Hamiltonian. With regards to the tolerance in the eigenvalues, we have set it to 10^{-14} allowing a maximum dimension of each Krylov space of 350 vectors. Were we in an exact situation, these vectors should be normalized to one and be orthogonal among themselves. Let us call V the matrix whose columns are these eigenvectors. We have checked that we obtain the following accuracy:

$$|{}^tVV - 1| \sim 10^{-4}, \quad (11)$$

which can be considered a low value for such a large number of eigenvectors. Moreover, as another check of the accuracy of the eigenvectors we have computed the total spin of each one of them and we have obtained integral values up to precisions of 10^{-6} in the vast majority of them. As for the invariance of the Hamiltonian under reflection with respect to the Ni atom, we have checked that symmetric one and two body correlators evaluated on every eigenvector are the same up to the fourth or fifth decimal digit.

In order to check how complete our set of eigenvectors is, we have compared the value at $t=0$ computed using Eqs. (5)

TABLE II. Relative error between the Ni self-correlation at $t=0$ using Eq. (5) with $M=400$ eigenstates and the value $\langle\psi_0|S^z_{\mathrm{Ni}}S^z_{\mathrm{Ni}}|\psi_0\rangle$ in the ground state, which is equal to 2/3.

J'	$C_{\mathrm{Ni}}(0)$	Error (%)
2	0.66666	0.00002
10	0.66666	0.0009
20	0.66653	0.02
30	0.66512	0.2
40	0.65660	2
50	0.57469	14

and (6) with the values obtained measuring the correlators in the ground state without the projectors in between. Table II shows these values and the relative error. It can be seen that the agreement is excellent for low values of J' while it goes worse for higher values of the coupling constant. At this point it is worth recalling that the accuracy of the dynamical Lanczos method can always be increased using more vectors of the Krylov subspace. In our case, retaining $m=400$ vectors and restricted to the chosen J' interval that we have studied, the errors stand within reliable limits and all the accuracy checks confirm that our numerical results are good enough so as to interpret them on physical grounds with respect to the spin frustration effects described in Secs. I–III.

B. Results

In Secs. I–III we have proposed and checked with the proper order parameters a static picture of the ground state of the Cr_8Ni ring. In the limit when the Ni is weakly coupled to the Cr bulk ($J'/J \ll 1$) the system is accurately described by an isolated Ni atom and an open Cr_8 chain. On the other hand, when the impurity is strongly coupled ($J'/J \gg 1$) the ring possess a dominant contribution in the form of a (2,1)-VBS ground state with some local correlations around the Ni atom due to the finite size of the sample. From the point of view of frustration, in this limit the impurity acquires strong antiferromagnetic compromises with both of its neighbors that cannot satisfy simultaneously. Frustration is known to impose complex constraints that can destabilize, deform, and even produce states of matter. On the other hand, the dynamics of each spin of the system is highly influenced by these constraints. In the following paragraphs we will see that the self-correlation of the Ni impurity and the rest of correlators with the Cr atoms allows us to naturally establish a relation with the amount of frustration.

In Figs. 6 and 7 we have plotted correlators (5) and (6) for a fixed value of the constant $J=16$ K and different values of J'. The Cr_8Ni ring is invariant under reflection with respect to the impurity site, and therefore we will only provide the correlators with the Ni itself and the Cr atoms numbered from 1 to 4 (with the notation of Fig. 2). The correlations with the Cr atoms numbered from 5 to 8 are the same as their symmetric counterparts. We want to provide these magnitudes with the meaning of a time-evolved probability, and hence we will consider only their modulus. It is worth noticing that the time correlators mentioned before at $t=0$ are real numbers, whereas for arbitrary values of t they are complex numbers. For convention, in the graphs where we plot the modulus of these correlators we will provide them with the same sign of their real value at $t=0$ to make explicit the

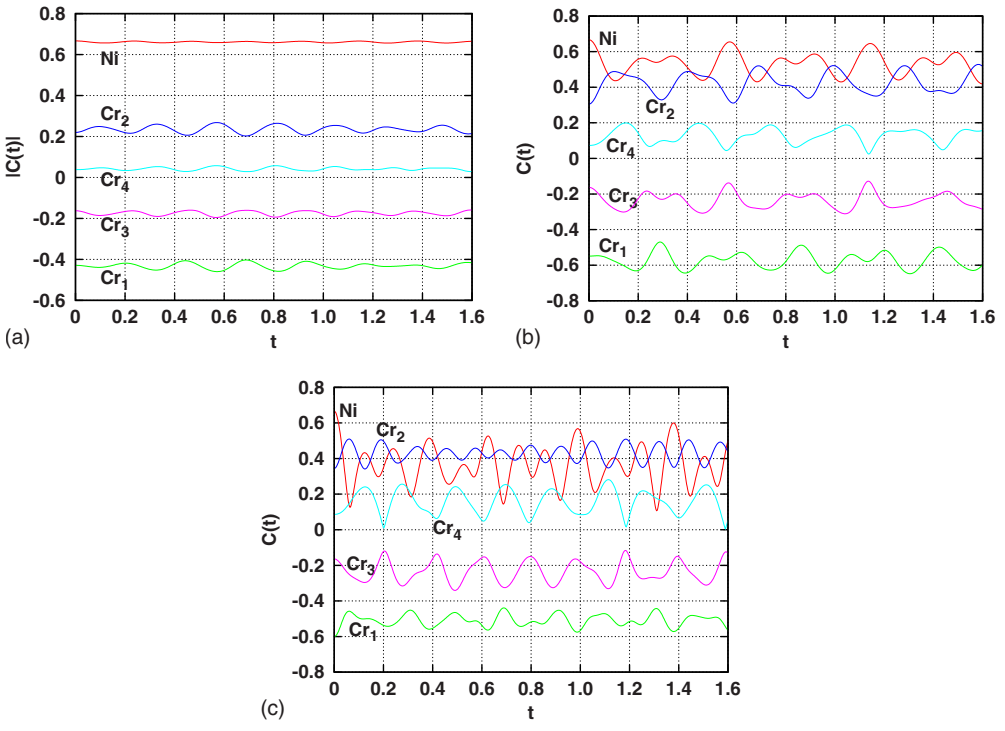

FIG. 6. (Color online) Modulus of the spin correlation of the impurity Ni atom with itself and with the rest of the Cr atoms. The graphs have been done with a value $J=16$ K and (a) $J'=2$ K, (b) $J'=10$ K, and (c) $J'=20$ K. For convention the sign of the correlators has been chosen to coincide with the sign of the correlation at $t=0$, which is a real number.

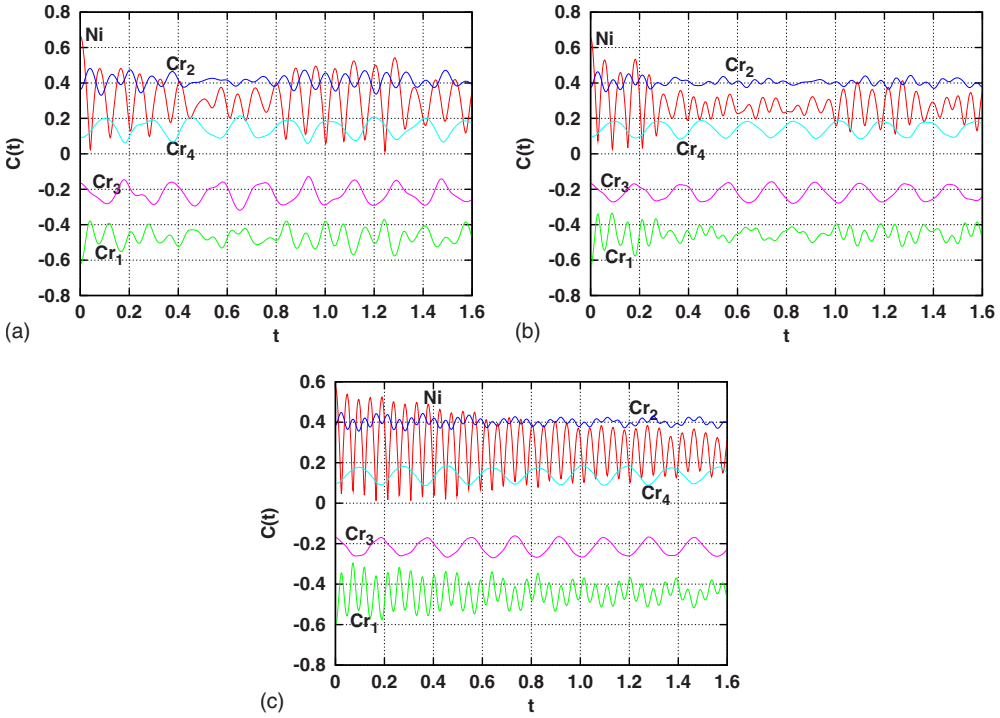

FIG. 7. (Color online) Modulus of the spin correlation of the impurity Ni atom with itself and with the rest of the Cr atoms. The graphs have been done with a value $J=16$ K and (a) $J'=30$ K, (b) $J'=40$ K, (c) $J'=50$ K. For convention the sign of the correlators has been chosen to coincide with the sign of the correlation at $t=0$, which is a real number.

ferromagnetic or antiferromagnetic nature that they possess in the static $t=0$ ground state.

In fact, we can observe in these graphs that the fingerprint of an antiferromagnetic order is present in the initial $t=0$ ground state and shows up in the alternation of the signs of the correlators. Notice also a signal of frustration in the fact that this alternation fails in the Cr_4 and its symmetric counterpart Cr_5 (due to the reflection invariance of the ring their value is equal with the same sign), where the correlations reveal that both spins are oriented in the same direction with respect to the spin of the Ni. Remarkably this ferromagnetic defect is a consequence only of the reflection invariance of the Hamiltonian.

From these graphs we can also infer that the average correlation of each spin with the impurity is little sensitive to the strength of the coupling constant J', although the amplitude of the deviations with respect to this average value increases with it. It can be also observed that the impossibility of the Ni atom to minimize its local interactions translates in relatively high correlations: in the coupling of spin 1 particle with spin 3/2 one can yield a total spin equal to 1/2, 3/2, and 5/2 with corresponding values of $\langle S_1^z S_2^z \rangle$ equal to $-5/6$, $-1/3$, and 1/2, while the computed correlations of the Ni with the Cr_1 are well above the minimum value $-5/6$.

The most important observation is that the dynamics of the correlators exhibit a nontrivial sort of periodicity. That is, from the shape of the curves it seems that there exist many modulating components but a dominant pattern of oscillations is apparent. Moreover, the frequency of this pattern clearly increases with increasing values of the impurity coupling J', i.e., as we move toward more frustrated regimes, but not in the same way for all the spins. We have captured in Fig. 8 the frequency of the dominant oscillatory pattern of each correlation. The graph highlights two different tendencies of the correlations depending on the considered spins: the frequency of the Ni self-correlation as well as the correlations of the Ni spin with the Cr_1 and Cr_2 spins increasing with J'. Moreover in the case of the Ni self-correlation the relation of these two variables is linear with a surprising accuracy. On the other hand the Cr_3 and Cr_4 are less affected

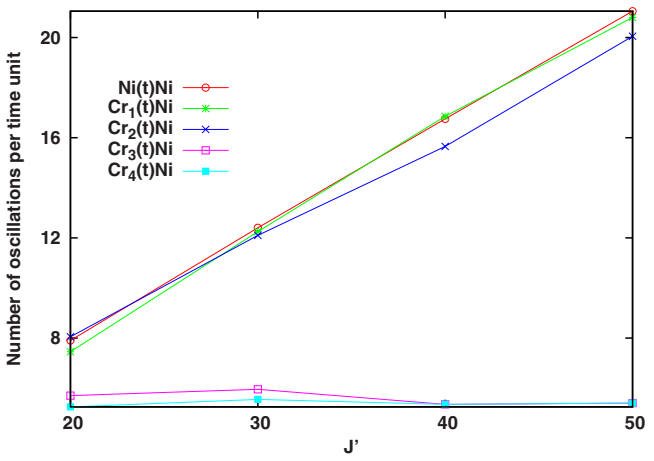

FIG. 8. (Color online) The number of oscillations has been obtained counting the number of minima in a wide time interval and dividing by the total time. The Ni, Cr_1, and Cr_2 have increasing frequencies with J' which corresponds to more frustrated regimes. In particular for the Ni spin the relation of these variables is linear up to a high precision. In the case of the Cr_3 and Cr_4 spins the frequency is hardly affected by J'.

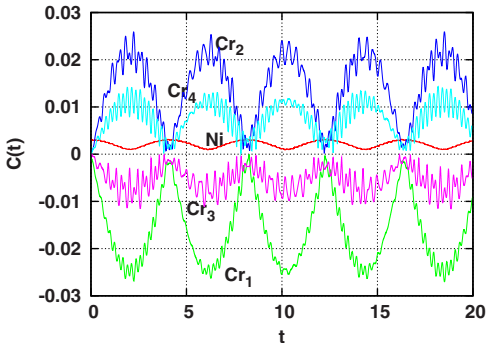

FIG. 9. (Color online) Modulus of the spin correlation of the impurity Ni atom with itself and with the rest of the Cr atoms. The values of the coupling constants are $J=16$ K and $J'=1$ K which corresponds to the region where the ground state is a triplet. For convention the sign of the correlators has been chosen to coincide with the sign of the correlation at $t=0$, which is a real number.

by the impurity spin and the frequency remains almost constant in the wide range considered.

In Fig. 9 we have plotted the same real-time correlations with an election of the coupling constants $J=16$ K and $J'=1$ K such that the ground state is a triplet. In this case the ground state is not rotationally invariant and the z-axis projection of the correlators is not proportional to scalar correlators (5) and (6). For our purposes however, these magnitudes suffice to realize the different nature of both the singlet and triplet ground states: first of all is that not one but two dominant patterns of oscillation are well distinguishable in the triplet regime. Second and also a major difference is that the scale in this regime is some orders of magnitude smaller than the singlet case.

The existence of this oscillatory behavior seems natural in a frustrated system where there does not exist a natural equilibrium position for each spin or where the resulting equilibrium configuration may result as unstable. In a system composed of classical spins these oscillations can be interpreted as the necessary movements of each spin to satisfy the frustrated interactions, becoming faster as we blur the concrete equilibrium positions with the frustrating interactions.

The results in Fig. 8 point toward a regime where the frustration introduced by the Ni impurity has strong local dynamical effects in the nearest and next-nearest Cr neighbors while the rest of the spins perceive the impurity screened by this closer shell of atoms, and therefore their dynamics is little affected by it. These results also show that the correlators proposed to study the frustration of the system indeed have the behavior expected for a suitable estimator in order to measure the intuitive idea we have about the amount of frustration in a certain system.

V. CONCLUSIONS

In recent years, considerable efforts have been devoted to synthesizing and investigating magnetic systems of nanoscale dimension that comprise a controllable number of transition-metal ions. Highly symmetrical clusters of almost planar ring shape are among such topical molecular nanomagnets. In particular, the bimetallic ring molecule Cr_8Ni is the first antiferromagnetic ring with an odd number of spins. Thus, it is a remarkable quantum system to test fundamental magnetic properties and, in particular, the spin frustration effects.

In this work, we have studied the Cr_8Ni frustrated ring in the regime where the ground state is a singlet. That is, with a fixed value $J=16$ K this region corresponds to $J'>1.5$ K. In this regard, the experimental characterization of a Cr_8Ni molecule places the real strengths present in the real system close to $J=16$ K and $J'=70$ K, well within the singlet region.

As we let the interaction strength of the Ni impurity be stronger than that between the Cr atoms, the ring stabilizes in a ground state with the quantum properties of a dimerized VBS. The picture that explains this behavior in terms of the possible bonds between neighbor particles comes clear from Fig. 2. Such a VBS state constitutes an example of a spin liquid with an intrinsic order that can be measured by means of some particular nonlocal order parameters. In Fig. 5 we show the computations of this order parameter on the ground state and its behavior supports neatly the VBS picture. In this regard, some finite-size effects can be observed in the order parameter that reveals a competition between the physics in the bulk of the ring and the strong effects, possibly mediated by the system frustration, which occurs in the vicinity of the Ni atom.

In Sec. II of this paper we have studied the role of the frustration in such a VBS state by means of computing the real-time evolution of the spin correlators between the atoms in the ring. In particular, we have found that the amount of frustration can be related to the frequency in the oscillatory behavior of this correlators. This relation can be naturally established from the observation that the oscillations in the system become faster as we move to the more frustrated regime $J' \gg J$. Such an oscillatory behavior is natural in a system where no natural equilibrium is allowed due to the frustration. However, the spin correlators reveal that the atoms that are most affected by this frustration are the Ni impurity itself and those Cr atoms that are closer to it, e.g., Cr_1 and Cr_2, while the effect of the impurity strength seems to be less influent in the Cr_3 and Cr_4 atoms. We believe that the methods and numerical techniques used in this work are versatile enough and can be extended to a variety of other nanomolecular magnetic compounds.

ACKNOWLEDGMENTS

Part of the computations of this work was performed with the High Capacity Computational Cluster for Physics of UCM (HC3PHYS UCM); funded in part by UCM and in part with FEDER funds. We acknowledge financial support from DGS grants under Contract No. FIS2006-04885 and the ESF Science Programme under Contract No. INSTANS 2005–2010.

[1] O. Cador, D. Gatteschi, R. Sessoli, A.-L. Barra, G. Timco, and R. E. P. Winpenny, J. Magn. Magn. Mater. **290-291**, 55 (2005).
[2] M. Allalen and J. Schnack, J. Magn. Magn. Mater. **302**, 206 (2006).
[3] D. M. Tomecka, V. Bellini, F. Troiani, F. Manghi, G. Kamieniarz, and M. Affronte, Phys. Rev. B **77**, 224401 (2008).
[4] S. Yamamoto and T. Hikihara, J. Phys. Soc. Jpn. **75**, 103701 (2006).
[5] H. Hori and S. Yamamoto, Phys. Rev. B **68**, 054409 (2003).
[6] J. Schnack and M. Luban, Phys. Rev. B **63**, 014418 (2000).
[7] F. K. Larsen, E. J. L. McInnes, H. E. Mkami, J. Overgaard, S. Piligkos, G. Rajaraman, E. Rentschler, A. A. Smith, G. M. Smith, V. Boote, M. Jennings, G. A. Timco, and R. E. P. Winpenny, Angew. Chem., Int. Ed. **42**, 101 (2003).
[8] S. Carretta, J. van Slageren, T. Guidi, E. Liviotti, C. Mondelli, D. Rovai, A. Cornia, A. L. Dearden, F. Carsughi, M. Affronte, C. D. Frost, R. E. P. Winpenny, D. Gatteschi, G. Amoretti, and R. Caciuffo, Phys. Rev. B **67**, 094405 (2003).
[9] M. Affronte, T. Guidi, R. Caciuffo, S. Carretta, G. Amoretti, J. Hinderer, I. Sheikin, A. G. M. Jansen, A. A. Smith, R. E. P. Winpenny, J. van Slageren, and D. Gatteschi, Phys. Rev. B **68**, 104403 (2003).
[10] I. Affleck, T. Kennedy, E. H. Lieb, and H. Tasaki, Phys. Rev. Lett. **59**, 799 (1987).
[11] I. Affleck, T. Kennedy, E. H. Lieb, and H. Tasaki, Commun. Math. Phys. **115**, 477 (1988).
[12] M. Fannes, B. Nachtergaele, and R. F. Werner, Europhys. Lett. **10**, 633 (1989).
[13] M. Fannes, B. Nachtergaele, and R. F. Werner, J. Phys. A **24**, L185 (1991).
[14] M. Fannes, B. Nachtergaele, and R. F. Werner, Commun. Math. Phys. **144**, 443490 (1992).
[15] A. N. Kirillov and V. E. Korepin, Leningrad Math. J. **1**, 343377 (1990).
[16] M. A. Martin-Delgado and G. Sierra, in *A Recurrent Variational Approach in Density-Matrix Renormalization, a New Numerical Method in Physics. Lecture Notes in Physics*, edited by I. Peschel, X. Wang, M. Kaulke, and K. Hallberg (Springer-Verlag, Berlin, 1999), Vol. 528, p. 91, and references therein.
[17] J. Gonzalez, M. A. Martin-Delgado, G. Sierra, and M. A. H. Vozmediano, in *Lecture Notes in Physics, Monographs* (Springer-Verlag, Berlin, 1995), Vol. 38, and references therein.
[18] M. Raczkowski and D. Poilblanc, arXiv:0810.0738 (unpublished).
[19] D. Gatteschi, R. Sessoli, and J. Villain, *Molecular Nanomagnets* (Oxford University Press, Oxford, 2006).
[20] J. Schnack, Lect. Notes Phys. **645**, 155 (2004).
[21] *Molecular Magnets: Recent Highlights*, edited by W. Linert and M. Verdaguer (Springer-Verlag, Vienna, 2003).
[22] M. den Nijs and K. Rommelse, Phys. Rev. B **40**, 4709 (1989).
[23] T. Kennedy and H. Tasaki, Phys. Rev. B **45**, 304 (1992).
[24] M. Oshikawa, J. Phys.: Condens. Matter **4**, 7469 (1992).
[25] J. Almeida, M. A. Martin-Delgado, and G. Sierra, Phys. Rev. B **77**, 094415 (2008).
[26] H.-H. Tu, G.-M. Zhang, and T. Xiang, arXiv:0807.3143 (unpublished).
[27] J. Almeida, M. A. Martin-Delgado, and G. Sierra, J. Phys. A: Math. Theor. **41**, 485301 (2008).
[28] M. Hagiwara, L. P. Regnault, A. Zheludev, A. Stunault, N. Metoki, T. Suzuki, S. Suga, K. Kakurai, Y. Koike, P. Vorderwisch, and J. H. Chung, Phys. Rev. Lett. **94**, 177202 (2005).
[29] E. R. Gagliano and C. A. Balseiro, Phys. Rev. Lett. **59**, 2999 (1987).
[30] E. R. Gagliano and C. A. Balseiro, Phys. Rev. B **38**, 11766 (1988).
[31] S. Haas, J. Riera, and E. Dagotto, Phys. Rev. B **48**, 3281 (1993).
[32] K. A. Hallberg, Phys. Rev. B **52**, R9827 (1995).
[33] K. A. Hallberg and C. A. Balseiro, Phys. Rev. B **52**, 374 (1995).
[34] J. Jaklic and P. Prelovsek, Phys. Rev. B **49**, R5065 (1994).
[35] J. Jaklic and P. Prelovsek, Phys. Rev. Lett. **74**, 3411 (1995).
[36] J. Jaklic and P. Prelovsek, Adv. Phys. **49**, 1 (2000).